

Analog VLSI Circuits for Adaptive Chemical Discrimination

Denise M. Wilson and Stephen P. DeWeerth*

School of Electrical Engineering, University of Kentucky,
453 Anderson Hall, Lexington, Kentucky 40506-0046 U.S.A.

(Received May 19, 1997; accepted February 23, 1998)

Key words: analog VLSI, electronic nose, smart sensors

We have designed and fabricated CMOS circuits that successfully discriminate between a variety of reducing chemicals in a manner resilient to concentration changes and other global variations in sensor response. The circuits described here use only six and seven transistors per chemical sensor to evaluate an array of sensory input based on the mean and median values of these inputs, respectively. Since these analog integrated circuits are constructed within a collective architecture, the mean and median values of the array of inputs are calculated in real-time, and each individual input is compared to the mean or median in parallel. The resulting output is a digital representation of the reducing chemical present in the sensing environment. When tested on a 15-element, heterogeneous array of tin oxide sensors, this hardware has proven sufficient to discriminate between five major reducing chemicals (acetone, butanol, ethanol, methanol and xylene).

1. Introduction

Over the past decade, the use of arrays to improve the selectivity of chemical microsensors has become increasingly popular, principally due to the poor selectivity inherent in many of these microsensors; a single sensor often yields poor performance for many discrimination tasks. To improve selectivity, many research efforts have turned to analyzing an array of chemical microsensors rather than a single sensor. For example, statistical analysis techniques have been used to analyze output from an array of sensors in order to improve discrimination capability. Techniques such as least squares method,⁽¹⁾ principal compo-

* Author currently with Georgia Institute of Technology, School of Electrical and Computer Engineering, Atlanta, Georgia U.S.A.

nent and cluster analysis,⁽²⁾ and decision-tree based pattern recognition⁽³⁾ have proven useful in improving this capability. Because of their ability to learn and recognize patterns in a robust manner, neural network analyses of chemical sensor arrays have also been used to perform many discrimination tasks over the last decade. Back propagation-trained⁽⁴⁻⁸⁾ and Kohonen⁽⁹⁾ neural networks have enjoyed substantial popularity in the analysis of arrays of chemical microsensors. All of these analysis techniques, that have been implemented in software, however, require the assistance of a digital computer to perform chemical discrimination, and operate on raw sensory data. Some application-specific hardware systems that perform these same discrimination tasks have also been developed in recent years.^(10,11) These systems employ conventional serial signal processing approaches using analog-to-digital converters, differential amplifiers and multiplexers. In this work, we have designed, fabricated and tested custom hardware that introduces pre-processing to an array of raw sensory input to assist in the pattern recognition process. The analog circuits presented here generate 15-element, binary patterns that are distinguishable for five reducing chemicals at various concentrations. The architecture and accompanying hardware are designed to be part of an integrated chemical analysis microsystem where sensors and circuits reside on a single chip. Further resolution and computational capability for sensory arrays using these pre-processing circuits can be achieved by finer selection of the temperature range under which the sensors operate and by similar careful selection of the types of sensors used in the array.

The hardware that we have designed may be used to analyze sensory output from a heterogeneous or a semi-heterogeneous array of chemical sensors. We define a heterogeneous array as one whose component sensors have different physical properties. The semi-heterogeneous array consists of chemical sensors whose physical properties (ad-desorption processes) are all the same but whose operating conditions (*e.g.* temperature) change across the dimensions of the array. The discrimination hardware that we describe here may be used with either the heterogeneous or the semi-heterogeneous array. In this work, we describe its performance in analyzing an array of discrete, heterogeneous tin oxide sensors to discriminate between various chemicals. The same hardware could be applied to a semi-heterogeneous array to make finer distinctions between members of the same or closely related families of chemicals.

The hardware described herein uses two thresholding algorithms implemented collectively in analog VLSI to convert an array of chemical sensory inputs into a digital representation. When this collective circuitry is implemented in an array of integrated chemical sensors, it will allow the circuits to be placed in physical proximity to the sensors themselves. One circuit or processing element per sensor ensures scalability to any size array and resolution; the local nature of collective hardware also assists in reducing the communication bottleneck at the chip I/O interface for a fully integrated chemical microsystem. Using thresholding algorithms based on the mean and median values in an array of sensory input, this smart sensor or smart pixel approach to processing sensory input, has already proven effective in image processing applications⁽¹²⁾ for evaluating regions of interest in a visual scene. In processing sensory input from an array of chemical sensors, this hardware may be used alone to accomplish simple discrimination tasks or as a preprocessing tool to generate robust input for more complex signal processing.

2. Materials and Methods

2.1 The thresholding algorithms

Conventional thresholding techniques have often used a fixed reference value as the basis for converting an analog image into a compressed digital representation of that image. Inputs that lie above or below this fixed reference generate a binary high or low output respectively. Mathematically, fixed thresholding can be expressed as follows:

$$f(i_n) = \begin{cases} 0 & \text{if } i_n < I_{\text{ref}} \\ 1 & \text{if } i_n > I_{\text{ref}} \end{cases} \quad (1)$$

where the quantity I_{ref} is a constant and i_n are the inputs. Fixed thresholding works well in environments where the global offsets and background levels of input are well known and controlled. When processing sensory input, however, this fixed thresholding technique can produce erroneous output images as global offsets in the sensory input change. In visual sensing tasks, such fixed thresholding might produce an accurate representation of a visual scene under indoor lighting, yet yield a completely white or binary high image in outdoor lighting. In chemical sensing, these global offsets can be a reflection of changes in concentration, drift, or ambient conditions. To accommodate global offsets, we propose adaptive thresholding techniques that remain insensitive to such global changes in a chemical image. The two reference values that we use for thresholding are the mean and median values in an array of sensory inputs. In an array of such inputs, thresholded according to the mean input value, any signal that lies above the mean value generates a binary high output from the thresholding circuitry. Likewise, any sensory signal that lies below the mean value generates a binary low output from this same circuitry. This algorithm can be expressed mathematically as follows:

$$f(i_n) = \begin{cases} 0 & \text{if } i_n < \frac{1}{N} \sum_k i_k \\ 1 & \text{if } i_n > \frac{1}{N} \sum_k i_k \end{cases} \quad (2)$$

where the inputs i_n are generated from the outputs of chemical sensors and N is the number of processing elements in the array. The value of N corresponds to the number of heterogeneous sensors in the array that are different from other sensors in the array. Inputs that lie above or below the mean generate a binary high or low voltage, respectively, at the output of their corresponding processing elements. In a similar manner, the algorithm for thresholding according to the median value in an array of inputs (where the number of inputs N is even) can be expressed as follows:

$$f(i_n) = \begin{cases} 0 & \text{if } i_n < \frac{1}{2}(i_{(N/2)} + i_{(N/2+1)}) \\ 1 & \text{if } i_n > \frac{1}{2}(i_{(N/2)} + i_{(N/2+1)}) \end{cases} \quad (3)$$

where the inputs i_n are first arranged in ascending order to properly calculate the median input value. The output is then a binary high or low value corresponding to input values above and below the median input value, respectively.

2.2 Implementations of mean and median thresholding techniques

Circuit implementations for mean and median thresholding are shown in Fig. 1. In both circuits, the input currents I_{in} are generated by applying the output voltage of a chemical sensor to the gate of the input transistor M_{in} . Ideally, an array of chemical sensors using

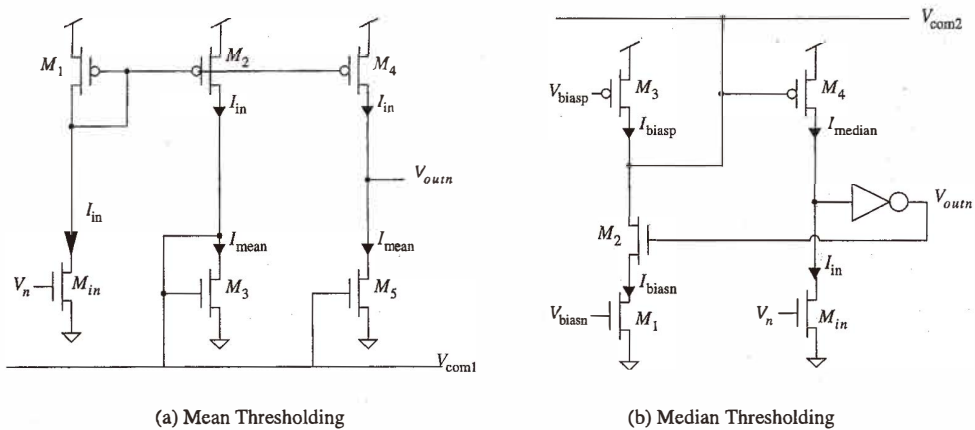


Fig. 1. Mean and median thresholding circuitry.

The above figure shows CMOS implementations of (a) mean and (b) median thresholding algorithms. In both cases, the input current I_{in} is generated by the transistor M_{in} with a sensor output voltage applied at its gate. Each heterogeneous sensor in the array contains one of these circuits to perform the processing for that sensor. In the mean thresholding circuit, the diode connected transistor M_3 carries the same current I_{mean} in every element in the array. These transistors are connected to every other processing element in the array through the node V_{com1} . The mean current I_{mean} is then compared to the input current I_{in} in the $M_4 - M_5$ comparator stage resulting in a high or low output for input currents lying above or below the mean respectively. Similarly, in the median thresholding circuit, the common node V_{com2} ensures that the sum of the bias currents I_{biasp} must equal the sum of the bias currents I_{biasn} . If the current I_{biasn} is set to $2I_{biasp}$, only $N/2$ of N circuit elements (with N an even number) can sink I_{biasn} . To maintain this equality, only half of the M_2 transistors in the array are turned on, resulting in a high output V_{out} at those processing elements that correspond to the highest valued inputs in the array.

these techniques would be part of an array of integrated processing elements or smart pixels, where a single processing element contains a chemical sensor and a mean or median thresholding circuit element depending on the algorithm implemented.

The mean thresholding circuit simply generates the mean current I_{mean} in the transistor M_3 and compares it to the input current I_{in} for every element in the array using the single-stage comparator formed by the $M_4 - M_5$ transistor pair. The mean current is generated by the remaining transistors in the circuit by first mirroring the input current to the transistor M_2 through the $M_1 - M_2$ current mirror. Here, the input current flows into the global common node, which is connected to the same point in every element in the array. At the common node, Kirchoff's current law must be satisfied as follows:

$$\sum_n I_n = \sum_n I_{\text{mean}} = NI_{\text{mean}}$$

$$I_{\text{mean}} = \frac{1}{N} \left(\sum_n I_n \right) = \text{mean current} \quad (4)$$

Thus, the transistor M_3 in every pixel conducts the mean current I_{mean} . The mean current is then compared to the input current I_{in} at every pixel through the $M_4 - M_5$ gain stage. The output V_{outn} is a binary high value if I_{in} is larger than I_{mean} , and a binary low if I_{in} is smaller than I_{mean} . To improve the consistency and gain of the output V_{outn} , the transistors M_4 and M_5 are lengthened to decrease the effects of process variation and transistor mismatch.

Using a similar approach, a seven-transistor circuit that thresholds inputs according to the median input value in an array of N elements is shown in Fig. 1b. To understand the operation of this circuit, first assume that the two bias voltages V_{biasn} and V_{biasp} are set such that I_{biasn} is equal to $2I_{\text{biasp}}$ when the bias transistors are both operating in saturation. Kirchoff's current law requires that:

$$\sum_n I_{\text{biasn}} = \sum_n I_{\text{biasp}} \quad (5)$$

Assuming that I_{biasn} is twice I_{biasp} , the transistor M_2 must be "turned off" (have a gate voltage equal to 0) in one half of the pixel elements, such that I_{biasn} does not flow in these elements. This restriction ensures that the I_{biasp} sum is equal to the I_{biasn} sum. The selection of elements which turn off I_{biasn} is made via the feedback from the output V_{outn} to M_2 . The pixels in which the transistor M_2 is turned on correspond to the highest input values in the array. If the input current, I_{in} , is large, the voltage V_{outn} rises, which turns M_2 on, sinking the current I_{biasn} for that element. Similarly, if I_{in} is small, V_{outn} falls, turning M_2 off, thereby preventing that pixel element from sinking I_{biasn} . If more or less than half the pixels attempt to generate binary high outputs, the common node voltage responds by decreasing or increasing, respectively, until the bias current balance is once again maintained.

2.3 Circuit results

Fifteen-element arrays of the mean and median thresholding circuits described in the previous section have been fabricated in a standard 2.0 μm , n-well CMOS process. Each

element occupies $5000 \mu\text{m}^2$ and $2000 \mu\text{m}^2$ for the mean and median thresholding elements, respectively. In both circuits, it is the current and not the voltage which is thresholded according to the mean and median. In subthreshold MOS transistor operation, where these circuits were tested, the current is exponentially related to the input voltage; this current-mode implementation has no effect on the median thresholding but creates a weighted rather than true mean of the sensor input voltages for the mean thresholding process. Small sensor outputs are given little weight in calculating the mean while large sensor outputs are given substantial weight. The result of the current-voltage conversion is that within the range of reacting sensors, the mean of the circuit is approximately proportional to the mean of these sensor output voltages (small signal region), while sensors that exhibit poor to no response are essentially eliminated from the calculation of the mean. This automatic outlier removal is suited to this chemical discrimination problem since sensors with little to no response do not contribute to the "chemical image" and should be ignored in evaluating relative responses of the sensor array.

Experimentally determined resolution of these circuits referenced to as input voltage are 0.02 V and 0.003 V for the mean and median thresholding circuits, respectively. These resolutions are at least 10 times higher than the resolution of the discrete tin oxide sensors used for these experiments (as specified by Figaro Eng, the manufacturer of these sensors).

2.4 Experimental setup for system testing

We have tested the mean and median thresholding hardware on an array of Taguchi sensors (TGS822, TGS813 and TGS880). The heterogeneous array consists of five of each type of sensor, where each operates at a different temperature, yielding a total of 15 sensors operating at five temperatures between 320 and 390°C; this temperature range is chosen for sensitivity to a broad range of chemicals and can be narrowed for a specific application or small subset of these chemicals. Each sensor is allowed to stabilize at its designated operating temperature for a week, after which the temperature is regulated by maintaining constant power across each sensor. The experimental setup for these experiments is shown in Fig. 2. Each tin oxide sensor (Fig. 2(a)) contains its own on-board heater. The heater temperature is maintained by a voltage regulator operating at a constant voltage with the result that it conforms to the desired temperature according to specifications provided by the manufacturer. The voltage regulator input is controlled with a precision, high current power supply. The tin oxide sensors used for these experiments consist of the following:

- Types of Sensors: 5 TGS822, 5 TGS813, 5 TGS880 (Figaro Eng)
- Sensor Sensitivity: TGS822 (reducing alcohols), TGS813 (ammonia), TGS880 (CO)
- Temperatures of Sensors: 5 temperatures evenly spaced between 320°C and 390°C
- Total Number of Sensors: 15 (fully heterogeneous)

For the fully heterogeneous array used to test the adaptive thresholding circuits, one voltage regulator is used to control three heaters each (one heater for each type of sensor). In this way, variations in the heater input for a particular operating temperature are minimized. Because the actual temperature of each sensor is independently controlled by the on-board heater, each sensor output is sensitive not only to variations in the actual sensor surface but also to variations in the heaters themselves. To be deemed robust, the outputs of the adaptive thresholding circuits should remain constant for a particular

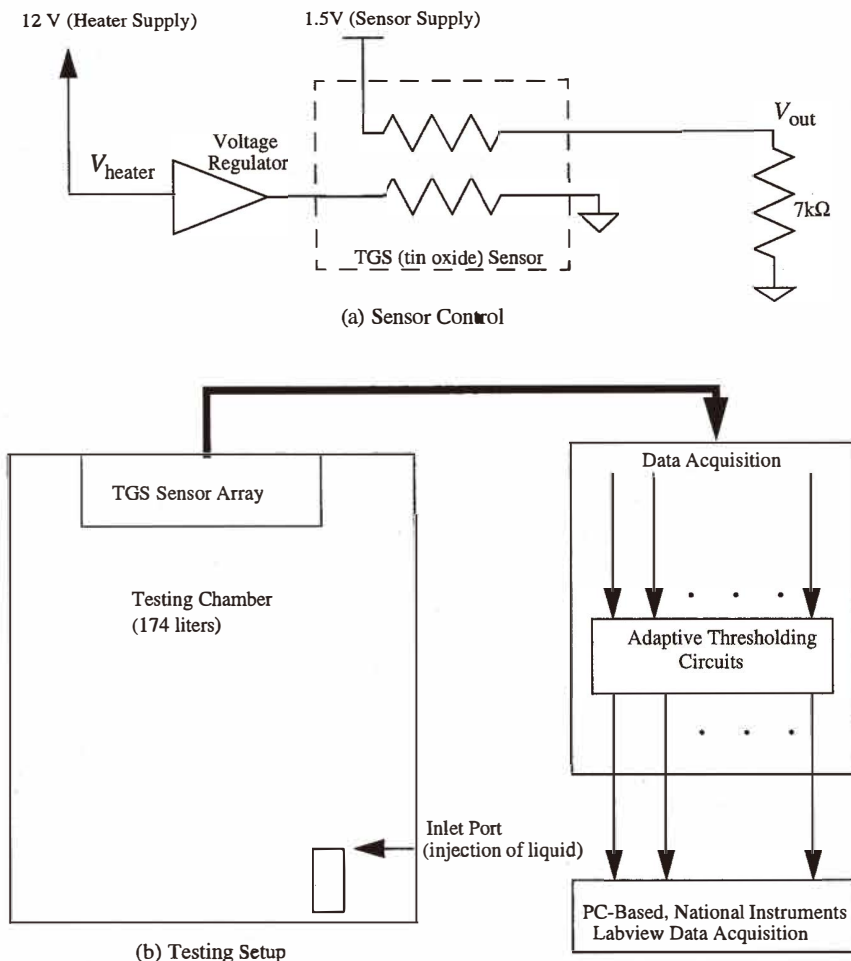


Fig. 2. Experimental setup for testing the adaptive thresholding circuits. Shown above is the testing setup for evaluating the performance of the adaptive thresholding circuits on an array of tin oxide sensors.

chemical not only in response to variations in the sensing environment and changes in the sensor material but, also, to changes in heater properties over the lifetime of the sensors. In integrated systems, additional circuitry can be added to maintain constant power rather than constant voltage to these sensors. The outputs of each sensor array are connected to the inputs of the appropriate processing circuits and the circuit outputs monitored by the Labview virtual instrumentation and data acquisition environment (National Instruments). Individual temperatures are controlled using voltage regulators at each sensor. All of the

sensors are allowed to stabilize for a week at the desired operating temperature before testing.

Various reducing chemicals are introduced in liquid form into a large testing chamber (Fig. 2(b)). The vapor from these liquids is allowed to diffuse without forced air flow up to the top of the chamber where the sensor arrays are mounted. The sensor outputs are monitored for approximately 10 minutes during their transient and steady-state responses. Even after the initial transient response, the outputs of the sensors continue to change as vapor continues to diffuse in the large testing chamber (174 liter chamber volume). After the testing period, the testing and evaporation chambers are aired for at least 30 minutes before the next test is performed. In the following sections, results for adaptive thresholding of the tin oxide sensor array inputs, previously described, are presented.

A typical output of the system described above is shown in Fig. 3. The output is a digital chemical image which is distinguishable from chemical to chemical and relatively invariant for a particular chemical. Each block of the output corresponds to a specific type of sensor (TGS822, TGS813, or TGS880) whose members operate at a specific temperature T . The white and black blocks correspond to a binary high output and a binary low output (V_{out}) respectively from the processing elements in the 15 element sensor array.

3. Results

Six different reducing chemicals were used to test the mean and median thresholding circuits. Complete responses from baseline to steady-state response for methanol in the 15 sensor array are shown in Figs. 4 and 5 as compared to the mean and median of each array respectively. It is apparent that consistent mean and median thresholded responses are best obtained from steady-state characteristics. The positions of sensors relative to the mean and median tend to switch for sensors close to the mean/median during the transient response of the sensors.

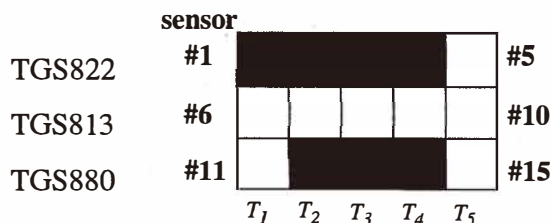


Fig. 3. Typical output response of the heterogeneous tin oxide smart sensor array.

A typical digital output pattern from the adaptive thresholding circuitry in response to sensory input from a heterogeneous array of tin oxide sensors is shown. The white and black boxes correspond to sensors that generate a binary high or binary low output at the corresponding circuit outputs respectively.

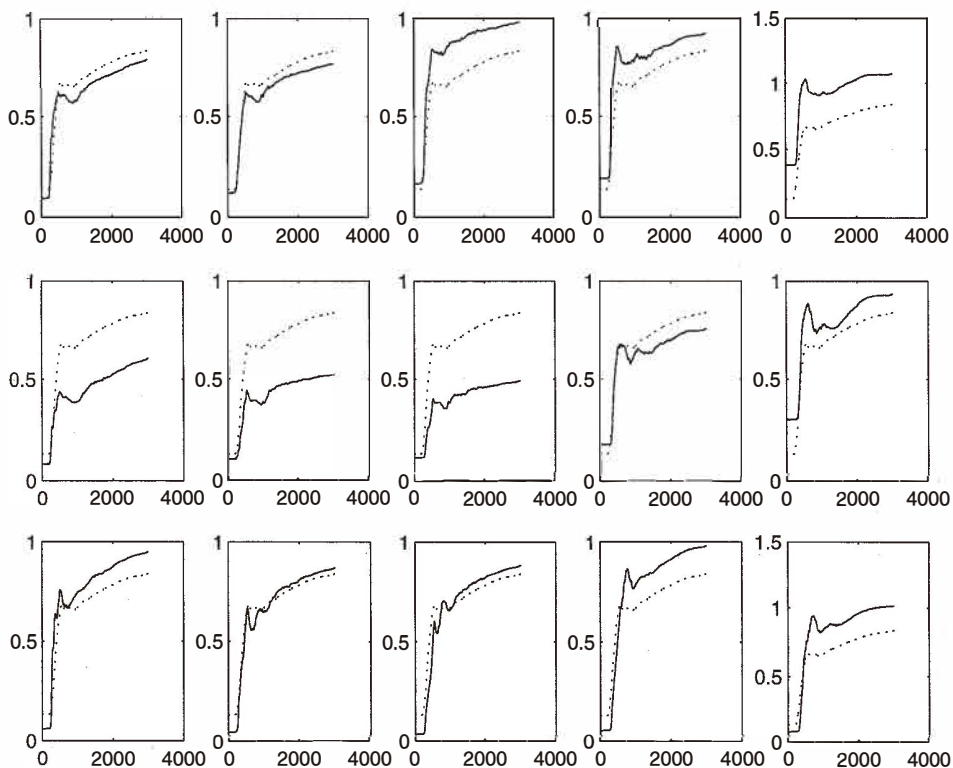


Fig. 4. Temporal responses of the sensor array relative to the mean.

Raw sensor output voltage vs time are shown as compared to the mean for the array at every timestep for methanol. The x-axis is time in 0.1 s intervals; the y-axis is output voltage of the sensors based on a 7 k Ω load resistance and a 1.5 V power supply. The dotted line is the mean value of the array.

As a result of these observations, experiments were performed only for steady-state responses of the 15-sensor array, after the initial temporal response had passed. Even then, ambiguous outputs were noted, especially in sensor #2, which was presumed faulty or nearing the end of its useful lifetime. Digital output patterns for the mean and median thresholding circuits are shown in Fig. 6 for six different reducing chemicals: acetone, butanol, ethanol, methanol, propanol, and xylene. In the figure, black represents a binary 0, white a binary 1 and gray undefined. Undefined outputs occur when the average value of that pixel over the 7 experiments of 500 data points each (3500 points total for each chemical) are ambiguous, defined as an average (binary) value between 0.2 and 0.8. In the experimental data taken for these six chemicals, note that eight pixels remain unchanged regardless of the chemical due to atypically high or low baselines (refer to Table 1) or

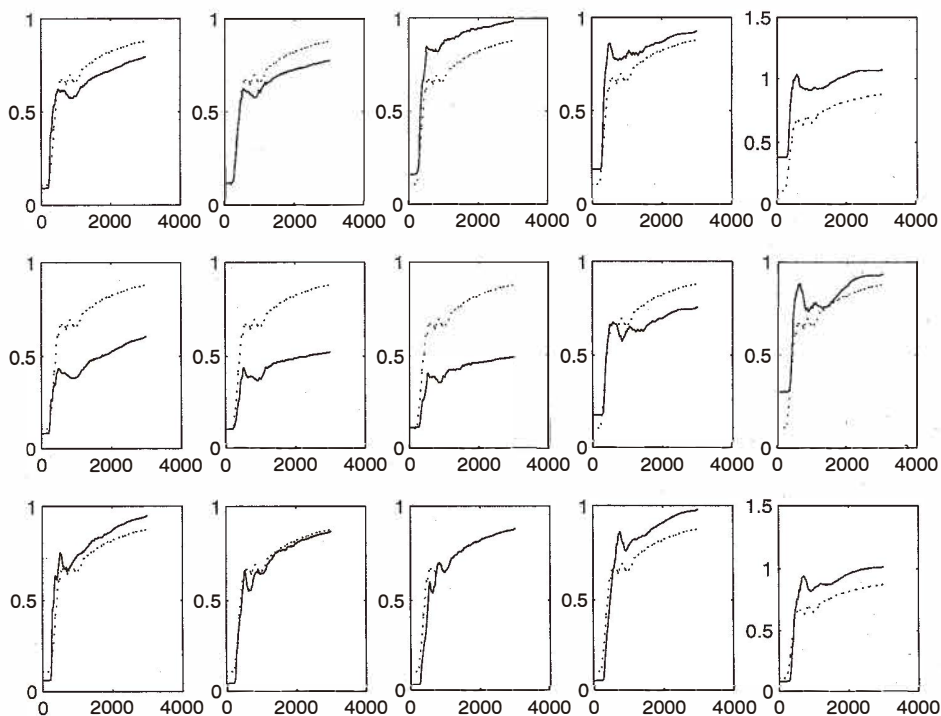


Fig. 5. Temporal responses of the sensor array relative to the median.

Raw sensor output voltage vs time are shown as compared to the median for the array at every timestep for methanol. The x-axis is time in 0.1 s intervals; the y-axis is output voltage of the sensors based on a 7 k Ω load resistance and a 5 V power supply. The dotted line is the median value of the array.

overall poor sensitivity of particular sensors to the chemicals tested. The resolution of the array could be better used by narrowing the temperature range to suit two or three chemicals of interest. The temperature range for these experiments remains broad in order to demonstrate the versatility and responsivity of the array. Further resolution could also be attained by eliminating the baseline conductance from the sensor output before thresholding. However, even without these improvements, the mean and median thresholding circuits distinguish 5 of the 6 chemicals tested, demonstrating the robustness of the adaptive thresholding approach. Atypically high baseline voltages (low baseline resistance) correspond to sensors at the highest operating temperatures. Although these baseline issues do not affect discrimination capability of the six chemicals tested, for more complex mixture and related chemical discrimination, these baseline issues would have to be removed from the thresholding process. In future work, we will begin to eliminate baseline effects from the thresholding process by using floating gate transistors or sample

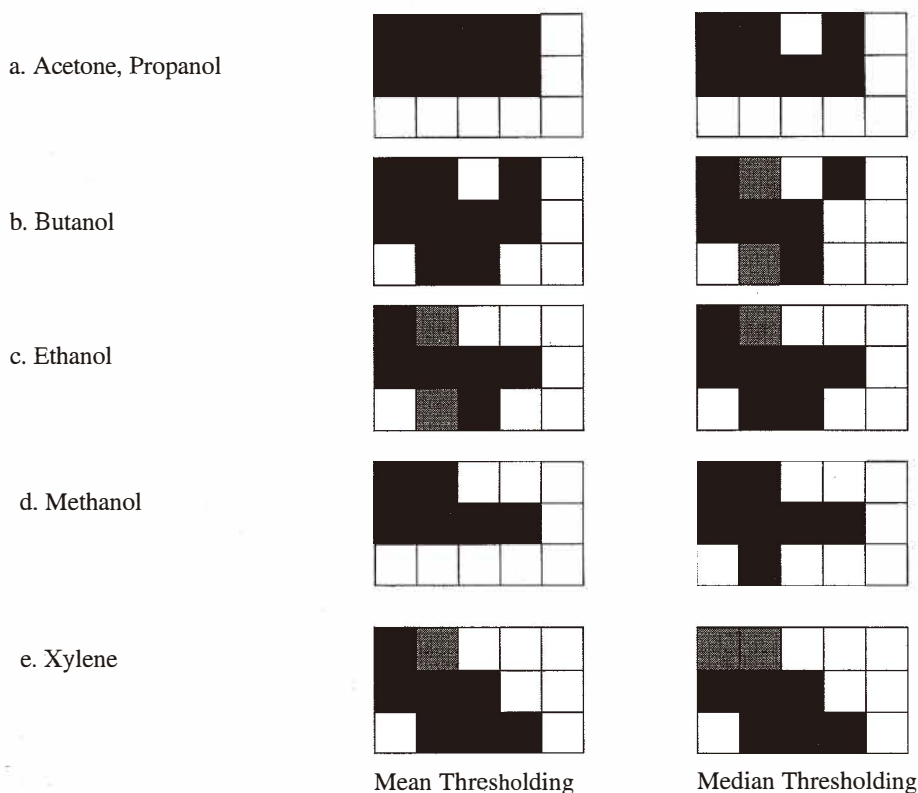


Fig. 6. Chemical output patterns.

Digital output patterns for the mean and median thresholding processes are shown above for six different reducing chemicals. Black represents a binary 0, white a binary 1, and gray undefined. Undefined occurs when, over the 90 sets of experimental data analyzed, the average value for that output (pixel) has an average value between 0.2 and 0.8. Note that 8 pixels remain unchanged regardless of the chemical, yet five chemicals remain distinguishable. With more sensors in the array and a temperature range tailored to particular applications, the use of these processing techniques can provide even higher resolution of chemicals and mixtures of chemicals.

and hold circuits to subtract baseline values from sensor outputs during the thresholding process. Additionally, as these tin oxide sensors are fabricated on microhotplates integrated into standard CMOS substrates and fabrication techniques, mismatch among their baselines will decrease, further minimizing baseline effects on the robustness of the thresholding process.

The adaptive nature of the both thresholding algorithms suggests that these digital chemical images should remain constant over changes in global parameters across the array such as concentration, drift, or ambient condition changes. As an example, the

images shown in Fig. 6 remain highly reproducible over 3500 points of experimental data taken for each chemical over a range of concentrations (500–3000 ppm) and humidity and other ambient conditions spanning two months of experimentation. As the concentration of a particular chemical changes or the sensor conditions change, the mean and median shift, allowing the output image to remain constant. This adaptability also makes the array output resilient to fluctuations in the sensing environment.

Typical baselines for these sensors in the middle of their testing lifetime are tabulated in Table 1. Atypically high or low baselines explain the consistently high or low values in the response images for the chemicals tested. Although discrimination of the gases presented in these experiments is still possible, removal of outliers, compensation for baselines, or replacement of outlying sensors is necessary to obtain maximum resolution of the array for discrimination of more chemicals and mixtures of chemicals. Without some form of baseline compensation, the mean and median thresholding techniques are limited, for a small number of sensors, in their ability to distinguish among many chemicals or vapors.

The chemical sensing array problem can borrow from the image processing community thresholding techniques that remove systematic characteristics of the array, such as baseline values, drift, and other background factors related to ambient and sensor conditions. Some more complex thresholding techniques such as global histogram-based thresholding, split and merge segmentation and thresholding, and smooth and threshold techniques traditionally used in image processing are also suitable for the multidimensional problem presented by chemical sensing arrays for vapor discrimination.⁽¹³⁾ In order to apply these more complex thresholding techniques to effectively approach chemical sensing problems using arrays of metal-oxide sensors, however, sensors have to be arrayed in such a way that spatial relationships are important and relevant to chemical discrimination. For portable, low-cost sensing nodes, the allowable complexity of implementations of these algorithms is limited; however, larger, multidimensional arrays of sensors, such as those potentially provided by a tin oxide sensing technology, provide sufficient sensory information that simple, carefully chosen algorithms can achieve the desired resolution at the sensing node level. For finer resolution, high accuracy systems, multiple sensing nodes or a software-based central processing center can apply more complex compression and thresholding algorithms. These types of signal processing architectures that combine simple compression algorithms in hardware with more complex algorithms in software

Table 1
Baseline resistances of sensor array.

Sensor	Baseline	Sensor	Baseline	Sensor	Baseline
1	0.113 V 86.1 k Ω	6	0.103 V 95.4 k Ω	11	0.085 V 117 k Ω
2	0.132 V 72.6 k Ω	7	0.122 V 79.4 k Ω	12	0.065 V 156 k Ω
3	0.167 V 55.9 k Ω	8	0.131 V 73.5 k Ω	13	0.053 V 192 k Ω
4	0.204 V 44.6 k Ω	9	0.191 V 48.1 k Ω	14	0.078 V 128 k Ω
5	0.320 V 25.9 k Ω	10	0.289 V 29.4 k Ω	15	0.113 V 86.1 k Ω

upstream of the hardware have already found substantial research attention and success in visual sensing and subsequent image processing.⁽¹⁴⁾ Similar benefits are expected from continued research in applying comparable signal processing architectures to chemical microsensing systems. The advantages of signal compression on the sensing plane when using arrays of sensors are primarily in lowered cost of the sensing node and increased bandwidth of useful information transferred to the user or next stage of signal processing.

Average values for 7 data sets (500 points per data set) for each chemical tested at an (estimated) concentration range of 500–3000 ppm and for each sensor value are shown in Table 2 and Table 3 for mean and median thresholding processes respectively. These average values represent the average of binary values after thresholding has taken place. In ideal median thresholding, the corresponding average values in Table 3 and Table 2 would be 1.00 for each “high” pixel and 0.00 for each “low” pixel. Effects of drift and noise however, cause the images in Fig. 6 to vary during experiments. Ambiguous values (shown as gray boxes in Fig. 6) are defined as those pixels generating an average value between 0.2 and 0.8 in these experiments. As discussed previously, compensation for baseline noise and variation among sensors can not only increase resolution by removing permanently “high” or “low” pixels but can also reduce noise in the thresholding process. Despite mismatch, inaccuracies, and drift in the 15-discrete-sensor array used in these experiments, 93% and 88% of the pixels were 80% reproducible or better for the mean and

Table 2
Average sensor pixel values after mean thresholding.

Chemical	1	2	3	4	5	6	7	8	9	10	11	12	13	14	15
Acetone	0.00	0.00	0.09	0.00	1.00	0.00	0.00	0.00	0.00	1.00	1.00	1.00	1.00	1.00	1.00
Butanol	0.00	0.17	0.91	0.00	1.00	0.00	0.00	0.00	0.36	1.00	1.00	0.17	0.17	1.00	1.00
Ethanol	0.00	0.59	1.00	0.88	1.00	0.00	0.00	0.00	0.00	1.00	1.00	0.50	0.16	1.00	1.00
Methanol	0.00	0.00	1.00	1.00	1.00	0.00	0.00	0.00	0.00	1.00	1.00	1.00	1.00	1.00	1.00
Propanol	0.00	0.00	0.00	0.00	1.00	0.00	0.00	0.00	0.20	0.91	1.00	1.00	1.00	1.00	1.00
Xylene	0.12	0.56	1.00	1.00	0.75	0.00	0.00	0.00	0.76	1.00	0.96	0.00	0.19	0.20	1.00

Table 3
Average sensor pixel values after median thresholding.

Chemical	1	2	3	4	5	6	7	8	9	10	11	12	13	14	15
Acetone	0.10	0.00	0.91	0.00	1.00	0.00	0.00	0.00	0.00	1.00	1.00	1.00	1.00	1.00	1.00
Butanol	0.00	0.51	1.00	0.00	1.00	0.00	0.00	0.00	0.83	1.00	1.00	0.47	0.20	1.00	1.00
Ethanol	0.00	0.67	1.00	0.93	1.00	0.00	0.00	0.00	0.00	1.00	1.00	0.31	0.12	1.00	1.00
Methanol	0.00	0.00	1.00	0.96	1.00	0.00	0.00	0.00	0.00	0.99	1.00	0.24	0.83	1.00	1.00
Propanol	0.00	0.00	0.44	0.00	1.00	0.00	0.00	0.00	0.57	1.00	1.00	1.00	1.00	1.00	1.00
Xylene	0.40	0.60	1.00	1.00	0.76	0.00	0.00	0.00	0.80	1.00	1.00	0.00	0.20	0.24	1.00

median thresholding processing respectively. Reproducibility problems are generally attributed to interference contributions from vapors previously introduced to the testing chamber and excessive noise in Sensor 2 (a near-“faulty” sensor).

4. Discussion

We have designed and fabricated hardware that thresholds an array of chemical sensor outputs into a digital representation based on the mean and median values of those outputs. Used alone, this hardware generates chemical images that vary in a sufficiently different manner among several related reducing chemicals to make discrimination among those vapors possible. Used as preprocessing tools, both adaptive thresholding techniques can also be useful for generating a more robust input for subsequent signal processing that can perform more complex discrimination tasks. Both as a stand-alone system and as a preprocessing tool, this adaptive thresholding approach is useful because it not only uses a minimal amount of hardware (6 or 7 transistors per sensor for the mean and median thresholding circuits respectively) but also because its digital output is resilient to changes in concentration levels and ambient conditions as well as to sensor mismatch. The nature of the hardware is such that it can easily be adapted to a variety of microsensor technologies in addition to the tin oxide sensors described here.

In future work, we plan to expand the resolution and number of sensors in our heterogeneous array to enhance the array's discrimination capabilities. In a long-term research effort, we hope to integrate the circuits and sensors onto a single substrate, thereby producing a single-chip chemical discrimination system. This thresholding hardware will also be applied to semiheterogeneous arrays to discriminate among more closely related chemicals within the same family. The long-term goal of this research is to produce single-chip, integrated chemical analysis microsystems that are sufficiently robust to perform tasks required by a range of consumer applications from breath alcohol analysis to seafood freshness detection.

Acknowledgment

The authors would like to thank MOSIS (MOS Implementation Service) for fabricating the VLSI circuits presented in this paper and the National Science Foundation for supporting Denise Wilson in her Ph. D. program.

References

- 1 H. V. Shurmer, J. W. Gardner and P. Corcoran: *Sensors and Actuators B* **1** (1990) 256–260.
- 2 J. W. Gardner: *Sensors and Actuators B* **4** (1991) 109–115.
- 3 B. Dulfer: *Eurosenors VIII*, Toulouse, France, Sept 26–28, 1994.
- 4 D. S. Vlachos and J. N. Avaritsiotis: *Eurosenors VIII*, Toulouse, France, September 26–28, 1994.
- 5 P. S. Barker, J. R. Chen, N. E. Agbor, A. P. Monkman, P. Mars and M. C. Petty: *Sensors and Actuators B* **17** (1994) 143–147.

- 6 J. W. Gardner, T. C. Pearce, S. Friel, P. N. Bartlett and N. Blair: *Sensors and Actuators B* **18–19** (1994) 240–243.
- 7 G. Niebling: *Sensors and Actuators B* **18–19** (1994) 259–263.
- 8 M. Holmberg, I. Lundstrom, F. Winquist, J. Gardner and E. Hines: Euroensors VIII, Toulouse, France, Sept 26–28, 1994.
- 9 F. A. M. Davide, C. Natale and A. D’Amico: *Sensors and Actuators B* **18–19** (1994) 244–258.
- 10 J. V. Hatfield, P. Neaves, P. J. Hicks, K. Persaud and P. Travers: *Sensors and Actuators B* **18–19** (1994), 221–228.
- 11 V. Demarne, B. Romanowicz, A. Grisel and J. Fournier: *Sensors and Actuators B* **18–19** (1994) 658–660.
- 12 T. G. Morris, D. M. Wilson and S. P. DeWeerth: 1995 *Advanced Research in VLSI* (IEEE Computer Society Press, Los Alamitos, California, 1995) pp. 241–255.
- 13 John C. Russ: *The Image Processing Handbook* (CRC Press: Boca Raton, Florida, 1995) Chapter 6.
- 14 Christof Koch and Hua Li, eds, *Vision Chips: Implementing Vision Algorithms with VLSI Circuits* (IEEE Computer Society Press: Los Alamitos, California, 1995).